

1 Article

2 **THROUGH THE LOOKING GLASS: Real time**  
3 **imaging in *Brachypodium* roots and osmotic stress**  
4 **analysis**

5

6 **Zaeema Khan <sup>1</sup>, Hande Karamahmutoğlu <sup>2</sup>, Meltem Elitaş <sup>2</sup>, Meral Yüce <sup>3</sup> and Hikmet Budak <sup>4\*</sup>**

7

8

9 <sup>1</sup> Molecular Biology, Genetics and Bioengineering Program, Faculty of Engineering and Natural Sciences,  
10 Sabancı University, Istanbul, 34956, Turkey11 <sup>2</sup> Mechatronics Program, Faculty of Engineering and Natural Sciences, Sabancı University, Istanbul, 34956,  
12 Turkey13 <sup>3</sup> Sabancı University SUNUM Nanotechnology Research Centre, Istanbul, Turkey14 <sup>4</sup> Cereal Genomics Lab, Department of Plant Sciences and Plant Pathology, Montana State University,  
15 Bozeman, 59717, USA

16 \* Corresponding author e-mail: hikmet.budak@montana.edu; Tel: 406-994-6717

17

18

19 **Abstract:** To elucidate dynamic developmental processes in plants, live tissues and organs have to  
20 be visualized frequently and for long time periods. The development of roots is studied in depth at  
21 a cellular resolution not only to comprehend the basic processes fundamental to maintenance and  
22 pattern formation but also study stress tolerance adaptation in plants. Despite technological  
23 advancements, maintaining continuous access to samples and simultaneously preserving their  
24 morphological structures and physiological conditions without causing damage presents  
25 hindrances in the measurement, visualization and analyses of growing organs including plant roots.  
26 We propose a preliminary system which integrates the optical real-time visualization through light  
27 microscopy with a liquid culture which enables us to image at the tissue and cellular level  
28 horizontally growing *Brachypodium* roots every few minutes and up to 24 hours. We describe a  
29 simple setup which can be used to track the growth of the root as it grows including the root tip  
30 growth and osmotic stress dynamics. We demonstrate the system's capability to scale down the  
31 PEG-mediated osmotic stress analysis and collected data on gene expression under osmotic stress.

32

33 **Keywords:** *Brachypodium*, neutral red, root, Casparyan bands, PEG-6000, osmotic stress, real time  
34 imaging, PDMS.

35

36

37

38

39

40

41

42

43

44

45 

## 1. Introduction

46 The understanding of development in plants as well as morphological dynamics occurring  
47 under stress conditions in plants requires a broad quantitative analyses of the tissue and cellular  
48 dynamics [1–3]. The *Brachypodium* root has emerged as a feasible model system to study cereals  
49 organogenesis since grain grasses have either huge roots, e.g. maize, multiple roots, e.g. wheat or  
50 specialized water conditions e.g. rice [4]. It offers various advantages for live imaging such as its  
51 simple architecture with a single primary axile root until 3 leaf stage, its moderate transparency, small  
52 size and steady growth rate [5,6].

53 Techniques based on high resolution imaging and fluorescence microscopy with automation  
54 have increased considerably but have faced short time span limitations in the past [7]. Recently  
55 several new studies have emerged introducing specialized platforms, device systems [8] and  
56 microfluidic chips which reduce labor, cost, increase observation time and provide automated high  
57 resolution imaging. Relevant examples of developmental and reproductive organ analysis were  
58 followed for several days in some cases [9,10]. Many studies have taken into account plant and  
59 plantlike organs such as fungal hyphae, pollen tubes, and developing roots by high resolution  
60 microscopy and analysed physical and physiological dynamics [9,11,12].

61 While the analyses of several plant organs, organogenesis, pattern formation, growth dynamics  
62 have been observed in microenvironments the structures observed have been at the cellular level  
63 with few dicotyledonous species observed table 1. There has been little manipulation of monocot  
64 grain seedlings in such systems partly due to the size, scale and morphological intricacies of most  
65 grasses. Monocotyledonous seeds are usually elliptical, slender long grains, with embryo polarity  
66 which makes the germination behaviour at the tissue and cellular level distinct from dicotyledons.

67 For analyzing temporal changes occurring under osmotic pressure and to maintain continuous  
68 imaging data during the stress application in developing seedlings, long term analysis in a suitable  
69 setup is a requisite. To allow such imaging the specimen must be constantly under nutrient supply  
70 while simultaneously uninterruptedly accessible for visualization. While several studies of young  
71 *Brachypodium* roots have been carried out [5,13] the real time optical imaging of developing roots  
72 under stress has not been reported so far, due to the aforementioned technicalities.

73 Polydimethylsiloxane devices offer several advantages to create platforms for manipulating  
74 thick tissues to subsequently allow for live imaging of cellular dynamics. These platforms can be  
75 created into desirable designs, size and tailor-made structures for the sample under observation to  
76 allow high throughput imaging data. These PDMS chips can be made into high resolution  
77 microfluidic chips to visualize cellular dynamics or molded into larger organ-on-a-chip for tissue and  
78 plant-on-a-chip for whole plant growth analysis [12,14]. To capture long term adaptations of plant  
79 roots to different microenvironments several root chip microfluidic platforms have also been  
80 introduced.

81 We developed a simple and preliminary yet enlightening setup to visualize real-time live  
82 imaging of growing *Brachypodium* seedling root at tissue level in temporal resolution for 24 hours.  
83 By utilizing the architecture and size of the root the platform has been specifically developed to  
84 acquire stress adaptation information of the root with minimal apparatus complexity and nominal  
85 hardware, creating an inexpensive setup with off-the-shelf optical parts. Therefore, our work is  
86 comprised of a simple optical microscopy adjusted to a novel growth and continuously observable  
87 system which can follow root development and osmotic stress dynamics in a continually growing  
88 monocotyledonous root.

89

90

91

92

93

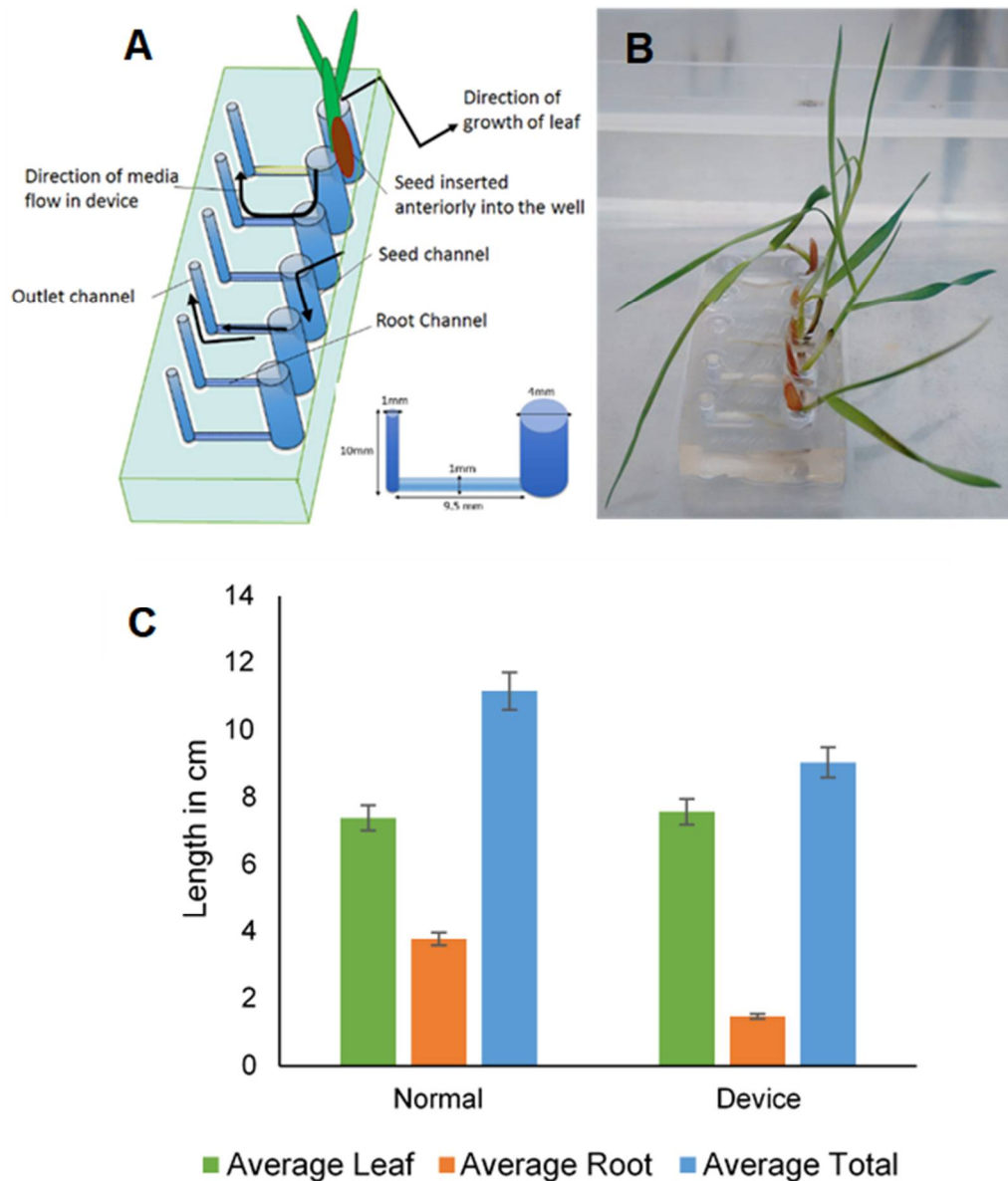
94

95

96 **2. Results**97 **2.1. Plant Growth in PDMS**

98 PDMS strips with single, double and triple punches were tested for compatibility with  
99 *Brachypodium* seedling growth, presented in Fig.S1. Single, double and triple punch channels had  
100 volume capacities of 130, 280 and 385  $\mu$ l, respectively. The growth compatibility and directionality  
101 observed in supplementary figure 1 C) provided initial data on how to handle the seed polarity in  
102 wells. Growth in was observed until the 3-leaf stage shown in E) which showed the plausibility of  
103 growing a grain seed relatively larger than *Arabidopsis* in a minimal quantity of growth media. In  
104 the 3-punch preliminary device with the 385  $\mu$ l MS media capacity, five weeks of growth inside the  
105 Petri plate was achieved by refilling the wells with unsolidified agar every week. Growth was  
106 observed until the formation of a small adult plant (6 leaf stage) and this observation was comparable  
107 to the plant-on-a-chip setup, reported previously for *Arabidopsis* [9].

108 Figure 1 shows the basic design of a channel-based platform extrapolated from the initial seed  
109 growth observed in Fig S1. The inset shows the dimensions of the channels to ensure growth in a  
110 single plane of focus. B shows the actual plantlet growth inside the device placed in a tissue culture  
111 box to maintain humidity. The channels were flooded with liquid MS media instead of solid MS  
112 media as in Fig S1. In this apparatus the average plantlet growth was observed and compared to  
113 normal growth as can be seen in C. Despite the root growth being lower than normal growth due to  
114 constrictions in 3D space the growth of leaves was the same as that in normal and overall growth  
115 observed was in parallel to normal growth.

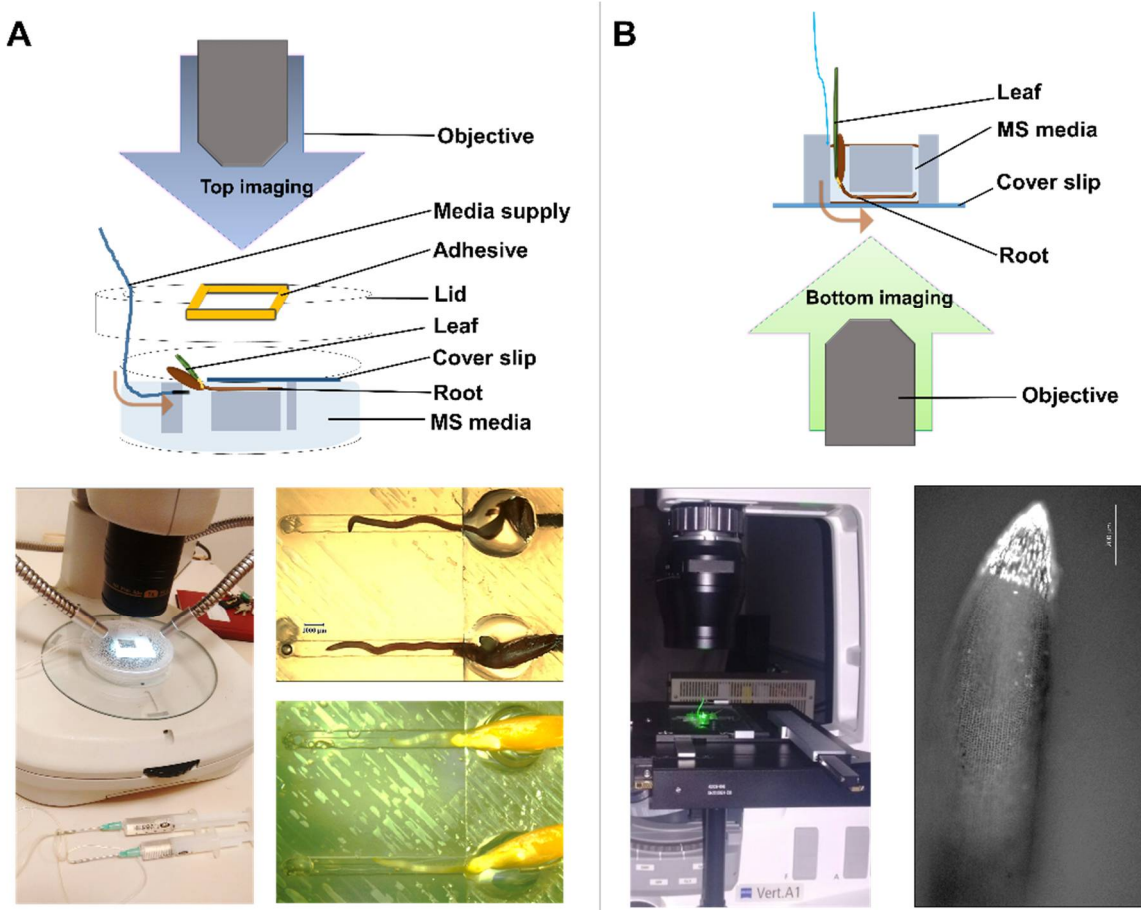


116

117 **Figure 1.** PDMS mold for growth and visualization analysis. The mold (A) used to construct the  
 118 PDMS plant chip device (B) and comparison of the leaf and root growth in solid MS media plates and  
 119 the plant chip device (C).

120 **2.2. Visualization Setups**

121 Figure 2 displays a detail of the images obtained from both the top and bottom imaging  
 122 arrangements. In A) as mentioned before due to the size of the monocot seed more than 2 parallel  
 123 experiments could not be observed simultaneously. However, the synchronous growth of 2 channels  
 124 was analyzed in the top setting. In A) the axial rotation and the growth constraint of the  $\sim 450\mu\text{m}$   
 125 diameter root inside a  $1000\mu\text{m}$  narrow channel can be visibly seen as curvatures and dents  
 126 throughout the length of the root in the non-stained image and more accurately in the neutral red  
 127 stained image. Fig. 2 B) shows the inverted fluorescent microscope focusing from the bottom  
 128 directly onto the coverslip of the device. The bottom imaging setting allowed the imaging of a single  
 129 channel at a time but nevertheless provided an accurate fluorescent signal for comparison of stress  
 130 and control samples.



131

132 **Figure 2.** Experimental setups for imaging. Top imaging (A) and fluorescent bottom imaging (B).  
 133 Three days-old seedlings having roots were mounted into wells for the top and bottom imaging. Top  
 134 imaging studies were conducted with a Nikon SMZ 1500 stereomicroscope (Japan) while the  
 135 fluorescent imaging studies were conducted with a Zeiss Axio Vert.A1 inverted microscope  
 136 (Germany).

### 137 2.3. Time Lapse Growth Curve Analysis in normal conditions and Root growth under PEG

138 The growth rate of three independent monocot seedlings in the plant chip device under 16h day  
 139 and 8h night conditions was observed with top imaging using the Nikon microscope Fig 3 A). The  
 140 24h time lapse video of *Brachypodium* seedlings was recorded at 24oC with a relative humidity of  
 141 37.5%. *Brachypodium* seedling roots showed slow growth with little change over time in the first 6  
 142 hours and then showed a slight increase in growth with a considerable increase in length during the  
 143 night hours. This observation could be due to negative phototropism in roots. It was observed as a  
 144 general trend that plant roots grow more rapidly in the dark hours as compared to the light hours as  
 145 seen in the graph from time point 20.00-4.00. A slight surge in root growth was observed in the early  
 146 morning hours followed again by a steady and continuous decrease. With time lapse recording, per  
 147 minute and per hour growth was recorded and the growth over 24 hours was also monitored. In the  
 148 plant chip device, the growth per minute was 4.3  $\mu\text{m min}^{-1}$ . The growth over a 24-hour period in  
 149 *Brachypodium* showed a similar trend to that seen in *Arabidopsis* in previous studies (Grossman et  
 150 al and Yazdanbakhsh et al). In the same setup 20% PEG-mediated osmotic stress was given and the  
 151 growth of the roots for 12 hours were observed (Fig 3 B and C). A drop in the growth of roots was  
 152 observed with almost continuous cessation of growth after 2-4 hours of osmotic stress as be downfall  
 153 trend in growth in  $\mu\text{m}$  in B, and a constant root length in C. The length of both seedlings showed  
 154 overall no growth under the osmotic stress. Since growth of the root showed a plateau after

155 approximately 4 hours, we choose 6 hours as a definite starting time point to observe stress under  
156 fluorescence for morphological changes in the root.

#### 157 **2.4. Root Cell Morphology and Horizontal Section Analysis**

158 Normal growth in the plant chip device was maintained for 72h (3DAG) after which the root  
159 was subjected to stress. After 6 hours of stress the device was placed on the fluorescent microscope  
160 stage for bottom imaging (see Fig 2B). Fig. 4 shows the longitudinal section of the maturation  
161 (differentiation) zone. In the normal root plant, we can see the endodermal cells brightly stained with  
162 neutral red and the Casparyan bands present. The root hairs and epidermal cells are not stained, and  
163 root hairs are dark extensions. In 6-hour, drought conditions we can see immediately the regulation  
164 of water intake by the Casparyan bands and their rigid square formation over the length of the root  
165 cells. These results are interesting as the vivid Casparyan bands depict increased suberization for  
166 increased water retention which causes them to be sharply visible under osmotic stress, the cell walls  
167 of the endodermis cells are vaguely visible underneath the Casparyan bands as is shown by the blue  
168 arrow (D).

169 The Casparyan bands prevent the high osmotic stress and negative water potential created by  
170 PEG-6000 to cause leakage of water from the stele figure B. Also, the growth of several lateral roots  
171 was observed in the stressed samples, indicating an adaptive behaviour of the cells to expand the  
172 space and surface area for further water uptake [15]. This behaviour of root hairs showing extensive  
173 growth was also observed after 18-hour osmotic stress on the root tips (Fig. 6 A and B). To confirm  
174 that the boundaries observed were of Casparyan bands which became compact and prominent  
175 around shrunken endodermal cells we observed the cells in a higher magnification after 24-hour  
176 stress (E & F). In the normal sample vacuoles were observed clearly in the root endodermal cells  
177 shown with arrow in E). In the 24-hour drought sample, the fluorescence signal was minimal with  
178 no vacuoles visible, and the staining of the Casparyan bands was not visible. Vague zones of  
179 fluorescence were observed (F, arrow), which could be lignin and suberin accumulation in Casparyan  
180 bands at 24 hours. Limited data could be acquired from the longitudinal section of the root after 24  
181 hours in 40x magnification thus to have a more precise and comprehensive view of suberin  
182 accumulation and cell morphology after 24-hour stress; we proceeded to prepare cross sections to  
183 understand which cells showed fluorescence after osmotic pressure.

#### 184 **2.5. Cross Section Analysis**

185 The cross sections of various zones across differentiation and elongation zones showed that the  
186 endodermis was stained and not the epidermis. This confirms the observation in Figure 4 that the  
187 compartments analyzed were of the casparyan tubes of the endodermis and not the epidermis. Figure  
188 5 shows the cross section of the *Brachypodium* root under unstressed and osmotic stress conditions  
189 after 24 hours. The most prominent changes can be observed in the root differentiation zone A-B and  
190 in the root elongation zone G-H). In the maturation zone, the vascular bundle shows visible  
191 shrivelling of their cells though the shrinking is more visible in B) as compared to D) and F). The  
192 metaxylem and protoxylem in A) appear larger and protruding. The endodermis desiccated around  
193 its periphery. A similar appearance of dehydrated cells was observed in D) and E) comparing to C)  
194 and E) The endodermis cells together with the vascular bundle and pith are condensed in D) and F).  
195 The zone of elongation with no clearly defined vessel cells. Also, there was no suberin or lignin  
196 increase observed in the epidermis since those zones remained unstained under PEG-mediated  
197 drought conditions. At the beginning of the elongation zone the fluorescence was considerably  
198 reduced showing that the place where the first sieve elements start to differentiate were affected by  
199 drought Fig 5 H). Overall the cross sections reveal abnormal morphology within the stele region of  
200 the sample under 24h osmotic stress induced by PEG. The morphology of the midsection of the root  
201 was also analyzed with and without fluorescence as seen in Supplementary Fig. 2. The confocal  
202 microscopy results conformed to our observations in Fig 5B). Furthermore, the observation of the  
203 Casparyan bands in Fig 4 B, D, F) was confirmed by the brightfield microscopy of the longitudinal

204 view of the stele. With neutral red the endodermis, stele was stained and not the outer part of the  
205 root or root hair.

## 206 **2.6. Root tip analysis**

207 In accordance with these results, Fig. 6 shows images of elongation zone cells obtained from  
208 plants under normal (A and C) and 24h osmotic stress conditions (B and D). An abnormal  
209 differentiation of the root cap hair was observed under brightfield imaging 18 hours after osmotic  
210 stress. This adaptation could be to increase surface area for improved water absorption. It is  
211 interesting to note that this observation could not be recorded in root stained with neutral red under  
212 brightfield (data not shown). On the other hand, a high fluorescent signal with bright and distinctly  
213 visible vacuoles appears to be higher in the root cap cells under standard growth conditions (C and  
214 E).

215 Under osmotic stress no fluorescence was observed in the root cap cells—which are the first sites  
216 of the plant in direct contact with the osmotic stress induced by the PEG molecules—as can be seen  
217 in Fig. 6 (D and F). The cell division zone shows fluorescence showing that under stress the  
218 meristematic zones increases its activity. Since neutral red is a vital dye for staining dead/alive  
219 regions its can be enough to state that illuminated regions under PEG stress depict mitotically active  
220 cells as in D).

## 221 **2.7. Plantlet Growth Maintenance**

222 In Fig 7 we analyzed the maximum extent to which we could maintain the *Brachypodium*  
223 plantlets inside the artificial setup environment. The graph shows the average growth of the plant's  
224 roots and shoots obtained from the array obtained from 26 seedlings after 1-month growth in PDMS,  
225 however extensive browning was observed at this stage thus we propose to analyze healthy green  
226 plantlets the experiment should not last more than 3 weeks. The average height of the leaf was  
227 recorded as 13 cm, average root length 1.63 cm, maximum shoot length of 22.5 cm and root length of  
228 2.6 cm was obtained after 4 weeks growth, which we propose as the maximum period to maintain  
229 the *Brachypodium* seedlings in the device (Fig. 7). Our purpose was to approach the maximum limit  
230 until the leaf senescence would start to manifest. The apparatus gives the potential of a plant-on-a-  
231 chip device. Furthermore, enough downstream applications such as stress application and RNA  
232 isolation for gene expression analysis.

## 233 **2.8. Gene Expression Analysis**

234 In order to have a broad idea of the plausibility of utilizing this artificial setup for genetic stress  
235 analysis several different genes were selected, 2 genes which are well established as upregulated, one  
236 was a predicted gene not experimentally validated, and 2 genes that were downregulated. No clear  
237 trend was observed at short term osmotic stress over a period of 2 hours. Since the expression pattern  
238 obtained for each gene was not definitive, we decided to proceed with greater osmotic stress over a  
239 longer period. 20% PEG was applied over a length of 24 hours. The data obtained were in line with  
240 previous expression profiles of the selected genes.

241 With more osmotic stress 20% PEG and longer stress duration (4, 6, 8, 12, 24 hours) the  
242 expression profile of upregulated and downregulated genes under water stress was similar to that in  
243 previous data. BdNAC54 and BdNAC92 were downregulated as has been previously reported [16].  
244 BdLEA5 is a gene upregulated in developing stages in plants, so its high expression was expected.  
245 DREB is a well-established drought responsive gene [17,18] and was upregulated at 4 hours and then  
246 displayed a 1.5 fold decrease at 6 hours and remained more or less the same until 24 hours. The most  
247 interesting observation was of the BdDi19 gene which is reported here the first time in *Brachypodium*  
248 *distachyon*. Its expression increased 120-fold after 24 hours of osmotic stress as seen in Fig 8.  
249 Dehydration-Induced 19 protein is a characterized protein in *Oryza sativa* having conserved domains  
250 in most grass species including *Aegilops tauschii*, *Hordeum vulgare*, *Setaria italica* among many

251 other Poaceae. This is the first time it has been experimentally verified to respond to drought in any  
252 plant species.

### 253 **3. Discussion**

254 Growth, directionality and compatibility was observed for *Brachypodium* seeds on all three  
255 PDMS punched molds and the results were in line with the previous reports conducted with  
256 *Nicotiana* and *Arabidopsis* [14,19,20]. After several experiments, we concluded that after 4 days of  
257 vernalization and 2 DAG seedling stage, the seedling had to be inserted in the correct orientation in  
258 the chip to make it grow along the length of the narrow 1mm channel. Growth was observed with  
259 the root penetrating the length of the microchannel with a slight curvature and bending.

260 A study on young wheat seedlings shows cell wall expansion in the maturation zone upon a low  
261 water potential around the roots and the authors suggest the accumulation of some solutes within  
262 the elongation and maturation zones in order to maintain the turgor pressure, resulting in an increase  
263 in the root diameter [21]. Although not seen in maturation zone cells, but a similar swelling behaviour  
264 of cells at the root apical meristem zone upon treatment with 5% PEG was previously reported for  
265 *Brachypodium* as well as wheat, rice, soybean, and maize [22], suggesting a collective response by  
266 root tissues of different plants to surmount the osmotic stress. The observation of Casparyan strips in  
267 the endodermis is in line with results on waterlogging in *Brachypodium* since both stagnant water  
268 and dehydration with PEG are osmotic pressures on the cells [13].

269 Our results show the ease of visualization and utilization of neutral red as a promising dye for  
270 monocot PEG mediated stress without tissue processing. Since Neutral red stains casparyan tubes it  
271 is an excellent vital stain to be used in monocots for in situ analysis without processing the tissue or  
272 sample preparation.

273 The Di19 protein was first reported in *Oryza sativa* as OsDi19-1 through RNA-Seq data. In  
274 *Triticum aestivum* it was known to have a C terminal domain. At the N terminus is a zinc finger zf-  
275 Di19. It was reported to be involved in environmental stress i.e. cold, drought, osmotic stress, and  
276 salinity. The protein was induced by high levels of abscisic acid and ethylene [23]. Though spatio  
277 temporal expression analysis the stem root and leaf overall showed an increase in expression of  
278 OsDi19 as compared to all other tissues (<http://ricexpro.dna.affrc.go.jp/GGEP/graph-view.php?featurenum=12093#tabs-2>). Under flooding and osmotic pressure, the expression also  
279 increased compared to other stress conditions such as salinity, cold, dryness, cadmium and hormones  
280 (<https://tenor.dna.affrc.go.jp/EPV/Os05t0562200-01/>). BdDi19 is thus a little-known gene which has a  
281 profound expression during short term osmotic stress in young seedlings. Further studies on this  
282 gene and protein in Poaceae could be useful in understanding dehydration and osmotic stress in  
283 relation to development.

284 This is the first study to incorporate neutral red for *Brachypodium* morphological analysis; this  
285 is also the first study to analyse PEG-mediated stress with neutral red dye. Moreover, this is the first  
286 study to experimentally validate Dehydration Induced 19 protein and analyse the expression levels  
287 of BdDi19 under drought stress.

288 We propose that a follow up study on *Brachypodium* seedlings in automated microfluidics or  
289 bioMEMS devices can be built upon our observations. Organ growth dynamics, root elasticity,  
290 microfluidic flow analysis and root hair dynamics under real time are a few of several areas which  
291 are desirable to be undertaken to unravel yet unknown physical patterns of growth and growth  
292 cessation and adaptation in favorable and stresses conditions.

### 294 **4. Materials and Methods**

#### 295 **4.1. Device fabrication**

296 Rectangular PDMS pieces with a scale of 65x20x10 mm single, double and triple punched with  
297 5 mm diameter punchers were initial seed growing reservoirs at different volumes to check  
298 biocompatibility. Acetone cleaned glass slides and PDMS pieces were plasma treated and bonded to  
299 get the final devices, which were used to test the compatibility of *Brachypodium* seeds with PDMS.

300 A mold for the plant chip was designed with SOLIDWORKS Software, reproduced onto ABS 3D  
301 material, and 3D printed. The mold dimensions were 10mm height, 9.5mm channel length, 1mm  
302 outlet diameter, and each seed channel 4 mm in diameter. The channel height was fixed at 1 mm to  
303 ensure the growth of the root to remain in one plane and not be out of focus in the Z-axis under  
304 microscopy as was earlier observed for 2mm channel width and height in Fig. 1.12. For the  
305 construction of the device, PDMS and curing agent were mixed in 10:1 ratio and poured into the mold  
306 in a 100-mm diameter Petri dish, degassed in a desiccator, and cured at 75 °C for 60 min in an oven.  
307 The PDMS pieces were cut and gently peeled off from the mold on the Petri dish. The constructed  
308 device was submerged in Murashige and Skoog media overnight to ensure the hardening of the  
309 device. 0.17 mm coverslips and the PDMS pieces were plasma treated and bonded to get the final  
310 devices. Coverslips were used instead of the glass slides to facilitate fluorescent imaging. This setup  
311 was fixed with an adhesive to the Petri plate cover. Each channel was filled with MS media.

#### 312 **4.2. Plant Imaging and growth chamber**

313 For each channel a seedling was grown in conventional petri plates with Murashige and Skoog  
314 solid media in closed and sterile conditions. The channel was designed to restrain the root growth to  
315 a horizontally narrow path (1mm diameter) which was optically transparent (0.17 mm glass  
316 coverslips). 4-days of vernalization and two days post-germination synchronously growing  
317 *Brachypodium* seedlings were inserted into the wells vertically at around 75-55° angle, with the  
318 scutellum facing slightly upwards and radicula facing downward to allow growth imaging of the  
319 roots in the horizontal narrow channels. The anterior end was immersed in the well, and the posterior  
320 end was entirely out of the well, with the emerging leaf facing outwards. This provided gas exchange  
321 and illumination for the leaves.

#### 322 **4.3. Seeds Preparation and Growth Measurement**

323 *Brachypodium* wild-type seed line Bd21-3 was used in this study. The seeds were dehusked then  
324 soaked in water for 10 minutes. They were sterilized for 1 minute with 70% ethanol in a sterile Petri  
325 dish. Ethanol was drained, and the seeds were rinsed with sterile deionized water. 20 ml of 1.3%  
326 NaOCl solution was poured into the Petri dish and rotated for 5 minutes. The seeds were then rinsed  
327 thrice with sterile deionized water. Ten seeds were placed in between two layers of sterile filter  
328 papers soaked in sterile water. After 4-day vernalization, the seeds were transferred to agar media  
329 and allowed to grow for 48h at 22oC with a 16h photoperiod and high relative humidity at 57%.  
330 Finally, the seedlings were transferred to the device. Epson perfection v700 photo scanner was used  
331 to visualise the full length of the seedlings grown in the microfluidic device and standard agar  
332 environment. WinRHIZO software (Regent Instruments, QC, Canada) was used to analyse the shoot  
333 and the root scan images (Fig. 1.12).

#### 334 **4.4. Imaging Setups**

335 Two different designs were developed for top and bottom imaging studies. The top imaging  
336 setup consisted of the same PDMS mold with the cover glass covering only the outlet channel, and  
337 the root channel, the seed channel was kept empty. This setup was then sealed with a double-sided  
338 adhesive tape to a carved-out Petri plate cover. The plate was filled with MS media and connected to  
339 syringes to ensure no air bubbles in the channels as well as constant media replenishment. For  
340 continuously monitored samples, the sample was illuminated from the above with a Nikon Fibre  
341 illuminator CFI-230 light source. The bottom setup consisted of the glass cover slip bonded to the  
342 entire device base to cover all the channels and the samples. Seeds were inserted anteriorly from the  
343 top with the root in the narrow horizontal channel. Fluorescent laser illuminated the sample from  
344 below through the glass coverslip.

#### 345 **4.5. Optical Apparatus**

346 The seedlings were selected at 2 days after germination (DAG) for microscopy studies. For  
347 standard visualisation of the control and stress samples, the device setup for top imaging was used.  
348 PEG-supplemented MS media was used for osmotic stress. The top imaging was performed using  
349 Nikon SMZ 1500, Olympus SZ61 stereo microscopes and illuminator lamp Olympus LG-PS2 from  
350 Japan. For bottom imaging of the samples with fluorescence, a stock solution of 4  $\mu$ M neutral red  
351 stain was prepared with 0.2X MS medium supplemented with 20mM potassium phosphate buffer at  
352 8.0 pH, according to the procedure reported earlier [24]. The control and stressed plantlet roots were  
353 stained for 15-20 minutes following the removal of PEG-supplemented MS media. The staining  
354 procedure made the cells stained under brightfield and enabled fluorescent visualisation of the  
355 seedling roots. Cross section samples were prepared according to the protocol described online [25].  
356 Fluorescence imaging was performed with Axio Vert.A1 inverted microscope by Carl Zeiss  
357 (Germany), using the bottom imaging setup. Confocal microscopy was performed with Carl Zeiss  
358 LSM 710, Germany and images recorded with Zen software (Carl Zeiss, Germany). Neutral red dye  
359 was used to visualize the live/dead parts of the roots of the young seedlings both for normal growth  
360 and for osmotic stress conditions. A single channel was used for visualisation with neutral red.  
361 Images were taken in 20X objective lens. Three-week old seedlings pre-stained with neutral red at the  
362 2-DAG (days after germination) seedling stage (stained as mentioned previously) were selected.  
363 These seedlings were given osmotic stress for 6 hours in Murashige and Skoog (full strength) media  
364 with 20% polyethylene glycol 6000. Stressed and normal seedlings were embedded in agarose (as  
365 described for the fluorescence microscope staining) to enable section slicing as thin as possible. Cut  
366 sections ~ 0.5-0.9mm were achieved from the maturation zone of the plant. Transverse sections were  
367 removed from the agarose molds and placed separately on acetone-ethanol cleansed cover slips and  
368 glass slides. The cover slips were sealed securely with clear nail polish.

#### 369 4.6. Imaging Acquisition

370 For continuous real time imaging acquisition the Nikon stereomicroscope SMZ 1500 was used  
371 together with the Nikon Fibre illuminator CFI-230 light source. Image acquisition was done with Spot  
372 Basic program. In the beginning of each experiment the root was positioned into focus. Samples were  
373 illuminated from above with 2 double arms and brightfield settings were used with 2 gain.  
374 Transmitted lower illumination was used for image capture in night hours. Imaging was carried out  
375 at 1X magnification due to the large size 420  $\mu$ m diameter non-transparent root. Image resolution  
376 was 1000 pixels per inch, sensor pixel size was 7.4x7.4  $\mu$ m, 68 sensor pixels were equal to 100 $\mu$ m.  
377 Imaging was set to occur every 5 minutes. The root rotation around all three axes during continuous  
378 growth was monitored by the stereomicroscope without need for repositioning or refocusing for 24  
379 hours. The day and night hours were maintained strictly and manually. Image acquisition was done  
380 by Spot Basic software. For normal growth curve 288 images were recorded for 24 hours to generate  
381 a time lapse video S1 video. The growth curve was generated by measuring every 12th image with  
382 the measurement settings in Spot Basic 4.7. For stress conditions the program was set to capture the  
383 image after every hour until 18 hours. Zen Blue program was used to acquire fluorescent and confocal  
384 imaging with manual image acquisition. For still imaging Fig S1 Kameran software was used  
385 manually in junction with the Olympus SZ61 stereo microscopes and illuminator lamp Olympus LG-  
386 PS2 (Japan).

#### 387 4.7. Osmotic Stress Application

388 To give osmotic stress 20% PEG 6000 was dissolved into the MS agar media and filled in the seed  
389 and root channel to three-week plantlets at the 3-leaf stage. For 6h and 24h osmotic stress analyses,  
390 the seedlings were first stained with neutral red for 20 minutes and then transferred to the  
391 microchannel device containing 20% PEG-MS and visualised under fluorescence microscope.

#### 392 4.8. Imaging for Osmotic Stress

393 For visualisation of growth, the model PDMS device was used in both dorsal and ventral  
394 positions. Top imaging was achieved by plasma bonding the glass to the dorsal side, but only  
395 covering the root channel and the outlet channel, leaving the seed channel open for insertion, as can  
396 be seen in Fig. 2 A. Petri plate was used for maintaining humidity and growth in which the radicula  
397 was inserted into the channel, with the coleoptile facing upwards and outwards and a gap created in  
398 the lid to ensure growth for the shoot. The coverslip was attached to the lid with a strong double-  
399 sided adhesive. The objective was positioned to focus directly on the cover glass and gap. Two holes  
400 were bored inside the lid to insert the valves for constant media flow. This entire setup was prepared  
401 aseptically under laminar flow hood. However, the seed part for shoot growth was kept uncovered  
402 during the length of the experiment. Media was inserted into the dish and into the device wells with  
403 the metal heads bored into the seed channel to ensure full media flow. The Petri plate lid and the  
404 bottom part was covered with paraffin film to ensure high humidity. The device could be maintained  
405 in this manner for 48h. The fluorescent bottom imaging was done with the entire ventral side of the  
406 device oxygen plasma bound to a glass coverslip. Seeds were inserted into the device with the  
407 coleoptile and radicula facing outwards and the bottom objective directly visualised the roots. The  
408 roots were separately stained with Neutral Red dye according to the protocol by Dubrovsky et al.  
409 [24] and rinsed in MS media and the channels filled with non-stained full strength MS media to avoid  
410 background. For fluorescence imaging 0.4  $\mu$ M neutral red solution and a 15-20 min incubation stained  
411 the roots sufficiently. 20% PEG was applied to full strength MS media for microscopic visualization  
412 of stress response morphological change of 2 DAG *Brachypodium* seedlings for 6, 18 and 24 hours.

#### 413 4.9. RNA isolation and DNase treatment

414 RNA isolation was done from the whole plantlets with a Zymo research kit MiniPrep RNA  
415 isolation kit. Briefly the tissue was homogenized in trizol reagent and transferred to column tubes.  
416 Flow through was DNase treated in the column, followed by prep buffer and wash buffers with  
417 intermittent centrifugations. The final eluted RNA was 20ul. The concentration of RNA was verified  
418 by nanodrop spectrometer. A bleach gel was used to analyse the integrity of the RNA. A 1% bleach  
419 gel was prepared in 1x TBE. 10X RNA loading buffer was used and a low molecular weight RNA  
420 ladder was used.

#### 421 4.10. Gene identification and primer design

422 From the plant genome database (<http://www.plantgdb.org/prj/GenomeBrowser/>) the  
423 *Brachypodium* genome was used to search for upregulated genes in drought. drought responsive  
424 family protein 19 (now renamed Dehydration Induced19) DI19, Late Embryogenesis abundant  
425 protein Lea5, sequences were downloaded, and primers designed. Primers for DREB2A were taken  
426 from Feng et al 2015. Two downregulated genes BdNAC054 and BdNAC092 were selected and  
427 primers taken from You et al 2015. Ubiquitin BdUBC18 was taken as internal Control and the primers  
428 used for it were also from You et al 2015. Primers used are listed in Supplementary Table 1.

#### 429 4.11. qRT-PCR

430 After confirmation of the integrity of the RNA samples, cDNA synthesis was performed with  
431 RevertAid First Strand cDNA Synthesis kit (Thermo Fisher Scientific, USA) following the  
432 manufacturer's instructions. Quantitative reverse transcription polymerase chain reaction (qRT-PCR)  
433 was performed by Light Cycler 480 System (Roche) using Perfecta SYBR Green Super Mix from  
434 Quanta. Amplification was performed in a total reaction volume of 10  $\mu$ l containing 5  $\mu$ l of 1X SYBR  
435 Green Super Mix, 300nM of each primer, and 100 ng of the template cDNA. The PCR thermal cycling  
436 parameters were set at 95oC for 10 minutes to activate the SYBR green followed by 40 cycles of 95 oC  
437 for 15 seconds and 60oC for 1 minute. For each sample, three technical replicates were made. Plant  
438 samples without stress treatment (0 hour) was used for normalization and fold change calculation.  
439 The  $\Delta\Delta Ct$  Pfaffel method was used to analyze the relative gene expression of the qPCR results.

440 **Supplementary Materials:** The following are available online at [www.mdpi.com/xxx/s1](http://www.mdpi.com/xxx/s1), Figure S1: title, Table  
441 S1: title, Video S1: title.

442 **Author Contributions:** HB, conceived the study. HB, ZK and MY designed of the study and drafted manuscript.  
443 HK designed the PDMS channel device. ME helped designing PDMS device. ZK carried out the all the  
444 experiments, analyses.

445 **Acknowledgments:** The authors acknowledge PhD candidate Soheila Zeinali (ARTORG Center for Biomedical  
446 Engineering Research, Organs-on-Chip Technologies, University of Bern, Switzerland) for fabrication of the  
447 preliminary 3-punch device.

448 **Conflicts of Interest:** The authors declare no conflict of interest.

#### 449 **References**

- 450 1. Nezhad, A.S.; Packirisamy, M.; Bhat, R.; Geitmann, A. In Vitro Study of Oscillatory Growth Dynamics  
451 of Camellia Pollen Tubes in Microfluidic Environment. *IEEE Trans. Biomed. Eng.* **2013**, *60*, 3185–3193,  
452 doi:10.1109/TBME.2013.2270914.
- 453 2. Gooh, K.; Ueda, M.; Aruga, K.; Park, J.; Arata, H.; Higashiyama, T.; Kurihara, D. Live-Cell Imaging and  
454 Optical Manipulation of Arabidopsis Early Embryogenesis. *Dev. Cell* **2015**, *34*, 242–251,  
455 doi:10.1016/j.devcel.2015.06.008.
- 456 3. Bennett, M.R.; Hasty, J. Microfluidic devices for measuring gene network dynamics in single cells. *Nat.*  
457 *Rev. Genet.* **2009**, *10*, 628–638, doi:10.1038/nrg2625.
- 458 4. Brkljacic, J.; Grotewold, E.; Scholl, R.; Mockler, T.; Garvin, D.F.; Vain, P.; Brutnell, T.; Sibout, R.; Bevan,  
459 M.; Budak, H.; et al. Brachypodium as a Model for the Grasses: Today and the Future. *PLANT Physiol.*  
460 **2011**, *157*, 3–13, doi:10.1104/pp.111.179531.
- 461 5. Hardtke, C.S.; Pacheco-Villalobos, D. The Brachypodium distachyon Root System: A Tractable Model to  
462 Investigate Grass Roots. In *Genetics and Genomics of Brachypodium*; Vogel, J.P., Ed.; Springer International  
463 Publishing: Cham, 2016; pp. 245–258 ISBN 978-3-319-26944-3.
- 464 6. Girin, T.; David, L.C.; Chardin, C.; Sibout, R.; Krapp, A.; Ferrario-Méry, S.; Daniel-Vedele, F.  
465 Brachypodium: a promising hub between model species and cereals. *J. Exp. Bot.* **2014**, *65*, 5683–5696,  
466 doi:10.1093/jxb/eru376.
- 467 7. Massalha, H.; Korenblum, E.; Malitsky, S.; Shapiro, O.H.; Aharoni, A. Live imaging of root–bacteria  
468 interactions in a microfluidics setup. *Proc. Natl. Acad. Sci.* **2017**, *114*, 4549–4554,  
469 doi:10.1073/pnas.1618584114.
- 470 8. Sena, G.; Frentz, Z.; Birnbaum, K.D.; Leibler, S. Quantitation of cellular dynamics in growing  
471 Arabidopsis roots with light sheet microscopy. *PLoS One* **2011**, *6*, 1–11, doi:10.1371/journal.pone.0021303.
- 472 9. Jiang, H.; Xu, Z.; Aluru, M.R.; Dong, L. Plant chip for high-throughput phenotyping of Arabidopsis. *Lab*  
473 *Chip* **2014**, *14*, 1281, doi:10.1039/c3lc51326b.
- 474 10. Busch, W.; Moore, B.T.; Martsberger, B.; Mace, D.L.; Twigg, R.W.; Jung, J.; Pruteanu-malinici, I.;  
475 Kennedy, S.J.; Gregory, K.; Nc, D. A microfluidic device and computational platform for high  
476 throughput live imaging of gene expression. *Nat. Methods* **2012**, *9*, 1101–1106, doi:10.1038/nmeth.2185.A.

477 11. Grossmann, G.; Guo, W.-J.W.-J.; Ehrhardt, D.W.; Frommer, W.B.; Sit, R. V.; Quake, S.R.; Meier, M. The  
478 RootChip: an integrated microfluidic chip for plant science. *Plant Cell* **2011**, *23*, 4234–4240,  
479 doi:10.1105/tpc.111.092577.

480 12. Bascom, C.S.; Wu, S.-Z.; Nelson, K.; Oakey, J.; Bezanilla, M. Long-Term Growth of Moss in Microfluidic  
481 Devices Enables Subcellular Studies in Development. *Plant Physiol.* **2016**, *172*, 28–37,  
482 doi:10.1104/pp.16.00879.

483 13. Shiono, K.; Yamada, S. Waterlogging tolerance and capacity for oxygen transport in *Brachypodium*  
484 *distachyon* (Bd21). *Plant Root* **2014**, *8*, 5–12, doi:10.3117/plantroot.8.5.

485 14. Meier, M.; Lucchetta, E.M.; Ismagilov, R.F. Chemical stimulation of the *Arabidopsis thaliana* root using  
486 multi-laminar flow on a microfluidic chip. *Lab Chip* **2010**, *10*, 2147, doi:10.1039/c004629a.

487 15. Paez-Garcia, A.; Motes, C.; Scheible, W.-R.; Chen, R.; Blancaflor, E.; Monteros, M. Root Traits and  
488 Phenotyping Strategies for Plant Improvement. *Plants* **2015**, *4*, 334–355, doi:10.3390/plants4020334.

489 16. You, J.; Zhang, L.; Song, B.; Qi, X.; Chan, Z. Systematic Analysis and Identification of Stress-Responsive  
490 Genes of the NAC Gene Family in *Brachypodium distachyon*. *PLoS One* **2015**, *10*, e0122027,  
491 doi:10.1371/journal.pone.0122027.

492 17. Hackenberg, M.; Gustafson, P.; Langridge, P.; Shi, B.J. Differential expression of microRNAs and other  
493 small RNAs in barley between water and drought conditions. *Plant Biotechnol. J.* **2015**, *13*, 2–13,  
494 doi:10.1111/pbi.12220.

495 18. Jiang, Y.; Wang, X.; Yu, X.; Zhao, X.; Luo, N.; Pei, Z.; Liu, H.; Garvin, D.F. Quantitative Trait Loci  
496 Associated with Drought Tolerance in *Brachypodium distachyon*. *Front. Plant Sci.* **2017**, *8*, 1–11,  
497 doi:10.3389/fpls.2017.00811.

498 19. Lei, R.; Qiao, W.; Hu, F.; Jiang, H.; Zhu, S. A simple and effective method to encapsulate tobacco  
499 mesophyll protoplasts to maintain cell viability. *MethodsX* **2015**, *2*, 24–32, doi:10.1016/j.mex.2014.11.004.

500 20. Ko, J.-M.; Ju, J.; Lee, S.; Cha, H.-C. Tobacco protoplast culture in a polydimethylsiloxane-based  
501 microfluidic channel. *Protoplasma* **2006**, *227*, 237–240, doi:10.1007/s00709-005-0142-2.

502 21. Akmal, M.; Hirasawa, T. Growth responses of seminal roots of wheat seedlings to a reduction in the  
503 water potential of vermiculite. *Plant Soil* **2004**, *267*, 319–328, doi:10.1007/s11104-005-0138-x.

504 22. Ji, H.; Liu, L.; Li, K.; Xie, Q.; Wang, Z.; Zhao, X.; Li, X. PEG-mediated osmotic stress induces premature  
505 differentiation of the root apical meristem and outgrowth of lateral roots in wheat. *J. Exp. Bot.* **2014**, *65*,  
506 4863–4872, doi:10.1093/jxb/eru255.

507 23. Li, S.; Xu, C.; Yang, Y.; Xia, G. Functional analysis of *TaDi19A*, a salt-responsive gene in wheat. *Plant*  
508 *Cell Environ.* **2010**, *33*, 117–29, doi:10.1111/j.1365-3040.2009.02063.x.

509 24. Dubrovsky, J.G.; Guttenberger, M.; Saralegui, A.; Napsucialy-Mendivil, S.; Voigt, B.; Baluska, F.; Menzel,  
510 D. Neutral red as a probe for confocal laser scanning microscopy studies of plant roots. *Ann. Bot.* **2006**,

511 97, 1127–38, doi:10.1093/aob/mcl045.

512 25. Schiefelbein Lab. Rapid Preparation of Transverse Sections of Plant Roots | Schiefelbein Lab Available  
513 online: <http://sites.lsa.umich.edu/schiefelbein-lab/rapid-preparation-of-transverse-sections-of-plant->  
514 roots/ (accessed on Apr 1, 2017).

515